Available online at http://scik.org
Commun. Math. Biol. Neurosci. 2026, 2026:71
https://doi.org/10.28919/cmbn/9881
ISSN: 2052-2541

BIFURCATION ANALYSIS AND OPTIMAL CONTROL OF AN SVITR COVID MODEL WITH VACCINATION AND TREATMENT STRATEGIES

SARLA CHOUHAN[1], ADITYA GHOSH[2,*], R. K. BHARDWAJ[2], SOUVIK KUNDU[3]

[1]Department of Applied Mathematics and Computational Science, SGSITS, Indore Madhya Pradesh-452003, India

[2]Department of Mathematics, Amity University, Kolkata-700135, India

[3]Department of Mathematics, Heritage Institute of Technology, West Bengal-700107, India

Abstract. This study proposes and analyzes a deterministic SVITR epidemiological model describing the transmission dynamics of COVID-19 incorporating vaccination and treatment strategies. The total population is divided into susceptible, vaccinated, infected, treated, and recovered compartments. Qualitative analysis of the model is performed to determine the disease-free and endemic equilibria and the basic reproduction number. Local stability of equilibria is examined using Jacobian analysis, while global stability is investigated using Lyapunov techniques. A bifurcation analysis is carried out to examine the qualitative changes in system dynamics near the critical threshold parameter. Sensitivity analysis is performed to identify the most influential parameters affecting disease transmission. Furthermore, an optimal control framework incorporating vaccination and treatment controls is developed using Pontryagin's Maximum Principle to minimize the number of infected individuals and intervention costs. Numerical simulations illustrate the theoretical findings and demonstrate the effectiveness of combined vaccination and treatment strategies in controlling the spread of COVID-19. The results highlight the importance of timely vaccination campaigns and effective treatment policies in mitigating epidemic outbreaks.

Keywords: COVID-19; SVITR model; bifurcation analysis; optimal control; vaccination; treatment.

2020 AMS Subject Classification: 92D30, 34D20, 49J15, 37N25

*Corresponding author

E-mail address: ghosh.aditya.iitg@gmail.com

Received March 15, 2026

1. INTRODUCTION

The Coronavirus, also known as severe acute respiratory syndrome coronavirus 2 (SARS-CoV-2), is a virus that mainly impacts the respiratory system. The disease caused by this virus is referredto as Covid-19 (Coronavirus Disease 2019). According to the ICTV Coronavirus Disease Study Group, this virus is closely related to severe acute respiratory syndrome. The first case of Covid-19 was detected in humans in December 2019 in Wuhan City, Hubei Province, China. The outbreak was officially announced as global health emergency or pandemic by the World Health Organization (WHO). The Chinese government enforced a quarantine in Wuhan City on January 23, 2020,aiming to reduce the pandemic's transmission. This action was noted by Hou C et. al in 2020. This disease possesses certain characteristics that have contributed to its extensive spread. It is caused by an RNA virus that can mutate and recombine rapidly as discussed by Markov et. all (Markov P.V et al. (2023)). It has a long incubation period, which means that people who are infected but asymptomatic can still spread the virus (Jiang X et al. (2020)); it is more deadly for certain groups, such as elderly individuals, immunocompromised persons, and individuals with pre-existing medical conditions as mentioned by Guan W. J. et al.(Guan W. J. et al. (2020)). It can be spread through droplets from coughing and sneezing, as well as contact with contaminated objects (Lotfi M. et al.(2020)). Vaccination is an important public health method in modern medicine, which has been used to reduce the impact of many infectious diseases demonstrated by Rappuoli R. et al.(Rappuoli R. et al.(2011)) and Moore S. et al. (Moore S. et al. (2021)). A vaccine refers to any material produced in terms of biology Which triggers a protective immune mechanism when administered to a susceptible individual. Vaccines assist the body in preparing to fight illnesses by leveraging the immune system's ability to recognize and resist infectious agents, such as viruses, bacteria, or toxins (Elgert K.D. (2009)). Rising worries exist that herd immunity may not be attained through vaccination due to the spread of more contagious variants, declining vaccine efficacy, and disparities in vaccine distribution. Vaccines reduce the likelihood of severe illness and death, therefore, widespread vaccination/immunization coverage is necessary to protect the healthcare system from overwhelming increases in infections. Getting vaccinated is a personal decision of social responsibility. However,the anxiety and negative side effects associated with the vaccine must

be addressed (Udolig M. etal. (2020)). Mathematical modeling is a useful technique for studying the spread of COVID-19 in several possibilities. It helps to predict the propagation of the disease over time by observing the population dynamics in different classes such as susceptible, infectious, recovered, and dead. There are different types of mathematical models, each with its own pros and cons (Bouchnita A. et al.(2020)). SIR (susceptible-infected-recovered) models are straightforward and offer rapid predic-tions. However, they may oversimplify the complexities involved in disease transmission (AlanaziS.A. et al. (2020)). In contrast, SEIR (susceptible-exposed-infected-recovered) models incorporatean additional exposed stage, making them more intricate but capable of providing a more preciserepresentation of disease dynamics (He S. et al. (2020)) and extended model was discussed byGhostine (Ghostine R. et al. (2021)). Building upon SEIR, SEIRD (susceptible-exposed-infected- recovered-dead) models introduce a compartment for individuals who have succumbed to the disease, enabling these models to capture the full progression of an epidemic, from onset to resolution (Loli Piccolomini E. et al. (2020); Fonseca I Casas P. et al. (2020)). This paper is organised as follows: Section 2 explains the considered model, while analysis of the model is discussed in next section. In Section 4, the stability analysis is presented and Section 5 emphasize primarily on numerical simulation. Section 6 illustrate the role of control on the model, section 7 describe the result and discussion of the whole work followed by conclusion in section 8.

2. Model Formulation

This model has been inspired by (Athithan, S. et al. (2013); Oshinubi, K. et al. (2023); Agbata, B. C. et al. (2019)) and gave inspiration to develop the mathematical model of COVID-19 with treatment class. In this study, Total population was divided by six compartments: susceptible $S(t)$, vaccinated $V(t)$, exposed $E(t)$, infected $I(t)$, treated $T(t)$, and recovered $R(t)$. The variables and parameters of the model are described in Table 1 and Table 2 respectively. It is important to recognize that individuals in the recovery class are neither contagious nor vulnerable to infection.

It is assumed in the model that the population is uniformly mixed, so each member is equally likely to come into contact with others. The parameter representing natural death rate is μ and rate of death related to COVID-19-related is δ.

After being vaccinated, susceptible individuals transition to the vaccinated compartment at a rate of α. Even so, the vaccinated population (V) can move back to the susceptible class with rate ρ due to vaccination inefficacy.

The COVID-19 virus can infect susceptible individuals at a rate of $\lambda = \beta SI$, where β represents the transmission rate between susceptible and infected populations.

After being infected, individuals shift to the exposed group (E), and exposed individuals move to the infected compartment and treatment class at rates ε and η, respectively. The remaining individuals shift to the recovery group due to strong immunity with rate τ. Infected individuals shift to the treatment group with rate γ, and treated individuals shift to the recovery group with rate ω.

We formulate the following system of nonlinear ordinary differential equations.

$$
\begin{aligned}
\frac{dS}{dt} &= \theta + \rho V - \beta SI - \alpha S - \mu S, \\
\frac{dV}{dt} &= \alpha S - \rho V - \mu V, \\
\frac{dE}{dt} &= \beta SI - \eta E - \varepsilon E - \tau E - \mu E, \\
\frac{dI}{dt} &= \varepsilon E - \gamma I - \mu I - \delta I \\
\frac{dT}{dt} &= \eta E + \gamma I - \omega T - (\mu + \delta) T \\
\frac{dR}{dt} &= \omega T + \tau E - \mu R,
\end{aligned}
\tag{1}
$$

The initial conditions of system (1) are,

$$
S(0) \geq 0, \quad V(0) \geq 0, \quad E(0) \geq 0, \quad I(0) \geq 0, \quad T(0) \geq 0, \quad R(0) \geq 0. \tag{2}
$$

Variables in the model	**Meaning**
S	Population which are Susceptible
V	Population which are vaccinated
E	Population which are exposed
I	Population which are infectious
T	Population which are Treated
R	Population which are recovered

TABLE 1. Notations used to describe different components

Parameters	Meaning of the notations
θ	Rate of inclusion of susceptible individuals
β	Transmission rate
ρ	vaccination rate
ε	Progression rate from exposed to active COVID-19
α	Vaccine Rate
η	rate from exposed to treated class
γ	Treatment rate of individuals with active COVID-19
ω	Rate of recovery among treated individuals
τ	recovery rate of exposed population
μ	Natural death rate
δ	Disease related death rate

TABLE 2. Defined parameters within the model and their significance.

3. ANALYSIS OF MODEL

This section provides positivity and boundedness for the solution variables described in equation (1).

3.1. Invariant region. We have obtained a domain where solutions of the system (1) are bounded uniformly within the region Δ of R^6.

Theorem 3.1. *The feasible solution set* $\Delta = \{S,V,E,I,T,R\}$ *of the system* (1) *with initial condition* (2) *then* $\Delta = \{S,V,E,I,T,R \in R^6_+ : S+V+E+I+T+R \leq \frac{\theta}{\mu}\}$ *is bounded region.*

Proof : In our model, we have considered whole population as

$N(t) = S(t)+V(t)+E(t)+I(t)+T(t)+R(t)$

$$\frac{dN}{dt} = \frac{dS}{dt}+\frac{dV}{dt}+\frac{dE}{dt}+\frac{dI}{dt}+\frac{dT}{dt}+\frac{dR}{dt} \tag{3}$$

$$\frac{dN}{dt} = \theta-\mu N-\delta I-\delta T \tag{4}$$

Without disease-induced death, then (4) becomes

$$\frac{dN}{dt} \leq \theta-\mu N$$

By integrating and for $t \to \infty$, we get the following equation

$$0 \leq N \leq \frac{\theta}{\mu}$$

Therefore, $\Delta = \{S,V,E,I,T,R \in R^6_+ : S+V+E+I+T+R \leq \frac{\theta}{\mu}\}$
is a positive invariant set for the system (1).

3.2. Positivity of Solutions: In order for the verification of system(1) to be epidemiologically significant and mathematically consistent, we need to demonstrate that every state variable is positive for every $t \geq 0$.

Theorem 3.2. *The solution corresponding to system* (1) *combined with the initial conditions* (2)*, is positively invariant for all* $t \geq 0$

Proof:Corresponding to (1), the following can be obtained from susceptible,

$$\frac{dS}{dt} = \theta + \rho V - \beta SI - \alpha S - \mu S,$$
$$\frac{dS}{dt} \geq -(\beta I + \alpha + \mu)S$$

implies

$$\frac{dS}{S} \geq -(\beta I + \alpha + \mu)dt$$

on integrating

$$\log S \geq -(\beta I + \alpha + \mu)t + C$$
$$S \geq e^{-(\beta I+\alpha+\mu)t}e^{C}$$

using initial conditions i.e.
at $t = 0$, $S = S_0$ therefore from above equation $S_0 = e^C$, where C is a constant, we get

$$S(t) \geq S_0 e^{-(\beta I+\alpha+\mu)t} \geq 0$$

Similarly we can verify that all the equations are positive for $t \geq 0$. Hence, theorem 3.2 is proved.

3.3. Equilibrium Point. There are two forms of equilibrium points: Disease-Free Equilibrium (DFE) Point, characterized by infected population $I = 0$,. The latter represent scenarios in which the disease persists in the population, at which $I \neq 0$, also referred as endemic equilibrium points (or outbreak equilibrium points).

3.4. Disease Free Equilibrium Point (DFE) (X^0): DFE (X^0) of the system (1) has been obtained by considering infection as zero. For DFE all classes that have infection will be considered as having zero infection. Therefore, DFE is.

$$X^0 = (S^0, V^0, E^0, I^0, T^0, R^0)$$

$$X^0 = \left(\frac{\theta(\rho+\mu)}{\mu(\alpha+\rho+\mu)}, \frac{\theta\alpha}{\mu(\alpha+\rho+\mu)}, 0, 0, 0, 0\right)$$

That describes a state where there is no infection present in the community.

3.5. Basic Reproduction Number. Spreading of the disease can be measured by Basic Reproduction Number(R_0), which is a crucial factor in determining whether COVID-19 will continue to spread within a population or disappear. It characterized the average number of secondary cases caused from a single infected susceptible individual (Fine, P. et al. (2011))..
One process of determining R_0 is by using the next-generation matrix method (Diekmann,O. et al. (2010)) after calculating by multiplying the F and $-V^{-1}$ matrices, where F represents transmission rate of infection between the E and I compartments and the matrix V accounts for other transfers between compartments.

$$F = \begin{pmatrix} 0 & \beta S^0 \\ 0 & 0 \end{pmatrix}$$

$$V = \begin{pmatrix} -(\eta+\varepsilon+\tau+\mu) & 0 \\ \varepsilon & -(\gamma+\delta+\mu) \end{pmatrix}$$

Therefore

$$K = F \cdot (-V^{-1}) = \begin{pmatrix} 0 & \beta S^0 \\ 0 & 0 \end{pmatrix} \begin{pmatrix} (\frac{1}{(\eta+\varepsilon+\tau+\mu)} & 0 \\ \frac{\varepsilon}{(\eta+\varepsilon+\tau+\mu)(\gamma+\delta+\mu)} & \frac{1}{(\gamma+\delta+\mu)} \end{pmatrix}$$

$$K = \begin{pmatrix} \frac{\varepsilon\beta S^0}{(\eta+\varepsilon+\delta+\mu)(\gamma+\delta+\mu)} & \frac{\beta S^0}{(\gamma+\delta+\mu)} \\ 0 & 0 \end{pmatrix}$$

The basic reproduction number is defined as the spectral radius of the next-generation matrix K. Thus, the basic reproduction number is given by:

$$R_0 = \frac{\beta \varepsilon S^0}{(\eta + \varepsilon + \tau + \mu)(\gamma + \delta + \mu)}$$

$$R_0 = \frac{\varepsilon \beta \theta (\rho + \mu)}{\mu(\eta + \varepsilon + \tau + \mu)(\gamma + \delta + \mu)(\alpha + \rho + \mu)}$$

3.6. Endemic equilibrium point EEP (X*). Let $X^* = (S^*, V^*, E^*, I^*, T^*, R^*)$ be the EE of the system of (1). we obtained EE by setting all the derivatives of the system (1) to zero, giving

$$\theta + \rho V - \beta SI - \alpha S - \mu S = 0 \tag{5}$$

$$\alpha S - \rho V - \mu V = 0 \tag{6}$$

$$\beta SI - \eta E - \varepsilon E - \tau E - \mu E = 0 \tag{7}$$

$$\varepsilon E - \gamma I - \mu I - \delta I = 0 \tag{8}$$

$$\eta E + \gamma I - \omega T - \mu T - \delta T = 0 \tag{9}$$

$$\omega T + \tau E - \mu R = 0 \tag{10}$$

solving these equation we get

$$S^* = \frac{\theta(\rho + \mu)}{\mu(\alpha + \rho + \mu)R_0}$$

$$V^* = \frac{\theta \alpha}{\mu(\alpha + \rho + \mu)R_0}$$

$$I^* = \frac{\mu(R_0 - 1)(\alpha + \rho + \mu)}{\beta(\rho + \mu)}$$

$$E^* = \frac{\mu(R_0 - 1)(\alpha + \rho + \mu)(\gamma + \mu + \delta)}{\varepsilon \beta(\rho + \mu)}$$

$$T^* = \frac{\mu(R_0 - 1)(\alpha + \rho + \mu)[\eta(\gamma + \mu + \delta) + \gamma\varepsilon]}{\varepsilon \beta(\rho + \mu)(\omega + \mu + \delta)}$$

$$R^* = \frac{\mu(R_0 - 1)(\alpha + \rho + \mu)[(\gamma + \mu + \delta)\{\omega\eta + \tau(\omega + \mu)\} + \omega\gamma\varepsilon]}{\varepsilon \beta \mu(\rho + \mu)(\omega + \mu + \delta)}$$

4. Stability Analysis

4.1. Local Stability for DFE. In order to evaluate the stability of the system represented by equation (1), the following results have been demonstrated.:

Lemma 1: The model will be locally asymptotically stable around DFE X^0, if $R_0 < 1$ and unstable when $R_0 > 1$.

Proof:Linearizing the system (1) around DFE,

$$J(X^0) = \begin{pmatrix} -(\beta I+\alpha+\mu) & \rho & 0 & -\beta S & 0 & 0 \\ \alpha & -(\rho+\mu) & 0 & 0 & 0 & 0 \\ \beta I & 0 & -(\eta+\varepsilon+\tau+\mu) & \beta S & 0 & 0 \\ 0 & 0 & \varepsilon & -(\gamma+\delta+\mu) & 0 & 0 \\ 0 & 0 & \eta & \gamma & -(\omega+\mu-\delta) & 0 \\ 0 & 0 & \tau & 0 & \omega & -\mu \end{pmatrix}$$

for X^0 system will be converted to

$$J(X^0) = \begin{pmatrix} -(\alpha+\mu) & \rho & 0 & 0 & 0 & 0 \\ \alpha & -(\rho+\mu) & 0 & 0 & 0 & 0 \\ 0 & 0 & -(\eta+\varepsilon+\tau+\mu) & 0 & 0 & 0 \\ 0 & 0 & \varepsilon & -(\gamma+\delta+\mu) & 0 & 0 \\ 0 & 0 & \eta & \gamma & -(\omega+\mu-\delta) & 0 \\ 0 & 0 & \tau & 0 & \omega & -\mu \end{pmatrix}$$

The characteristics equation is given

$$J(X^0) = \begin{pmatrix} -(\alpha+\mu)-\lambda & \rho & 0 & 0 & 0 & 0 \\ \alpha & -(\rho+\mu)-\lambda & 0 & 0 & 0 & 0 \\ 0 & 0 & -(\eta+\varepsilon+\tau+\mu)-\lambda & 0 & 0 & 0 \\ 0 & 0 & \varepsilon & -(\gamma+\delta+\mu)-\lambda & 0 & 0 \\ 0 & 0 & \eta & \gamma & -(\omega+\mu-\delta)-\lambda & 0 \\ 0 & 0 & \tau & 0 & \omega & -\mu-\lambda \end{pmatrix}$$

the determinants gives

$$\{-(\alpha+\mu)-\lambda\}\{-(\rho+\mu)-\lambda\}\{-(\eta+\varepsilon+\tau+\mu)-\lambda\}\{-(\gamma+\delta+\mu)-\lambda\}$$
$$\{-(\omega+\mu+\delta)-\lambda\}\{-\mu-\lambda\} = 0$$

hence $\lambda_1 = -(\alpha+\mu)$

$\lambda_2 = -(\rho+\mu)$

$\lambda_3 = -(\eta+\varepsilon+\tau+\mu)$

$\lambda_4 = -(\gamma+\delta+\mu)$

$\lambda_5 = -(\omega+\mu+\delta)$

$\lambda_6 = -\mu$

since $\lambda_1, \lambda_2, \lambda_3, \lambda_4, \lambda_5, \lambda_6 < 0$, then the model is stable around DFE.

4.2. Global Stability around DFE. Lemma 2: The disease-free equilibrium point X^0 is globally asymptotically stable if $R_0 < 1$.

Proof: To prove the global stability of the disease-free equilibrium, the Lyapunav function below is constructed:

$L = B_1 E + B_2 I$

Where

$B_1 = (\gamma + \mu + \delta)$

$B_2 = \beta S$

$$L = (\gamma+\delta+\mu)E + (\beta S^0)I$$

$$\frac{dL}{dt} = (\gamma+\delta+\mu)\frac{dE}{dt} + (\beta S^0)\frac{dI}{dt}$$

$$\frac{dL}{dt} = (\gamma+\delta+\mu)\left[\beta S^0 I - (\gamma+\varepsilon+\tau+\mu)E\right] + \beta S^0\left[\varepsilon E - (\gamma+\delta+\mu)I\right]$$

$$\frac{dL}{dt} = \left[\beta\varepsilon S^0 - (\gamma+\delta+\mu)(\gamma+\varepsilon+\tau+\mu)\right]E \quad (11)$$

$$\frac{dL}{dt} = \left[\frac{\beta\varepsilon\theta(\rho+\mu)}{\mu(\alpha+\rho+\mu)} - (\gamma+\delta+\mu)(\gamma+\varepsilon+\tau+\mu)\right]E$$

$$\frac{dL}{dt} = (\gamma+\delta+\mu)(\eta+\varepsilon+\tau+\mu)\left[\frac{\beta\varepsilon\theta(\rho+\mu)}{\mu(\alpha+\rho+\mu)(\gamma+\delta+\mu)(\eta+\varepsilon+\tau+\mu)} - 1\right]E$$

$$\frac{dL}{dt} = (\gamma+\delta+\mu)(\eta+\varepsilon+\tau+\mu)[R_0 - 1]E < 0 \text{ if } R_0 < 1$$

Hence $\frac{dL}{dt} < 0$ if $R_0 < 1$

If $E = 0$ then $\frac{dL}{dt} = 0$

Therefore, according to Lasalles' invariance principle, the system exhibits global asymptotic stability.

4.3. Sensitivity Analysis of the model for DFE.

4.4. Sensitivity Analysis of the Basic Reproduction Number. Sensitivity analysis helps to determine the relative importance of different parameters in influencing the basic reproduction number R_0. It identifies which parameters have the greatest impact on disease transmission and can therefore guide effective control strategies.

The normalized forward sensitivity index of R_0 with respect to a parameter p is defined as

$\Upsilon_p^{R_0} = \frac{\partial R_0}{\partial p} \times \frac{p}{R_0}$.

Using the above definition, the normalized sensitivity indices for each parameter are calculated as follows.

$$\Upsilon_\beta^{R_0} = 1$$
$$\Upsilon_\varepsilon^{R_0} = \frac{\eta+\tau+\mu}{\eta+\varepsilon+\tau+\mu}$$
$$\Upsilon_\theta^{R_0} = 1$$
$$\Upsilon_\rho^{R_0} = \frac{\rho}{\rho+\mu} - \frac{\rho}{\alpha+\rho+\mu}$$
$$\Upsilon_\alpha^{R_0} = -\frac{\alpha}{\alpha+\rho+\mu}$$
$$\Upsilon_\eta^{R_0} = -\frac{\eta}{\eta+\varepsilon+\tau+\mu}$$
$$\Upsilon_\tau^{R_0} = -\frac{\tau}{\eta+\varepsilon+\tau+\mu}$$
$$\Upsilon_\gamma^{R_0} = -\frac{\gamma}{\gamma+\mu+\delta}$$
$$\Upsilon_\delta^{R_0} = -\frac{\delta}{\gamma+\mu+\delta}$$

A positive sensitivity index indicates that an increase in the parameter value will increase the basic reproduction number R_0, thereby enhancing disease transmission. Conversely, a negative sensitivity index implies that increasing the parameter value will reduce R_0 and help in controlling the spread of the disease. We can see the impact of parameter on the Basic reproduction number as per the Sensitivity Index Table.

Parameter	Value	Sensitivity Index
β	0.45	1
θ	10	1
ε	0.30	0.72
ρ	0.20	0.08
α	0.25	-0.21
η	0.15	-0.11
τ	0.10	-0.07
γ	0.35	-0.26
δ	0.05	-0.03
μ	0.02	-0.18

TABLE 3. Sensitivity Index Table

4.5. Bifurcation Analysis around DFE. To investigate the qualitative behavior of the model near the disease-free equilibrium (DFE), we analyze the system using bifurcation theory. In particular, we determine whether the system exhibits a forward or backward bifurcation when the basic reproduction number R_0 crosses the critical threshold value $R_0 = 1$.

Let β be the bifurcation parameter associated with the transmission of infection. The disease-free equilibrium of the system is given by

$$E_0 = (S^*, V^*, 0, 0, 0, 0)$$

where

$$S^* = \frac{\theta(\rho+\mu)}{\mu(\alpha+\rho+\mu)}$$
$$V^* = \frac{\alpha S^*}{\rho+\mu}$$

In this section, we investigate the qualitative behavior of the system near the disease–free equilibrium (DFE). The center manifold theory developed by Castillo-Chavez and Song is used to determine the direction of bifurcation that occurs when the basic reproduction number crosses unity. Using the next generation matrix method, the basic reproduction number is obtained as

$$R_0 = \frac{\beta S_0}{\gamma+\mu+\tau}$$

The critical threshold occurs when $R_0 = 1$, which implies

$$\beta = \beta_c = \frac{\gamma+\mu+\tau}{S_0}. \tag{12}$$

Let $w = (w_1, w_2, w_3, w_4, w_5)^T$ be the right eigenvector satisfying $J(E_0)w = 0$.

Solving the above system yields

$$w = \left(-\frac{\beta S_0}{\mu}, 0, 1, \frac{\tau}{\mu+\delta}, \frac{\gamma(\mu+\delta)+\tau\delta}{\mu(\mu+\delta)}\right)^T.$$

Let $v = (v_1, v_2, v_3, v_4, v_5)$ be the left eigenvector satisfying $vJ(E_0) = 0$.

The normalized left eigenvector is obtained as $v = (0, 0, 1, 0, 0)$

with normalization condition $v \cdot w = 1$.

Following the center manifold theory, the bifurcation coefficients are defined as

$$a = \sum_{k,i,j} v_k w_i w_j \frac{\partial^2 f_k}{\partial x_i \partial x_j}(E_0) \tag{13}$$

and

$$b = \sum_{k,i} v_k w_i \frac{\partial^2 f_k}{\partial x_i \partial \beta}(E_0). \tag{14}$$

After computation of the second-order derivatives, we obtain $a = -\frac{2\beta S_0}{N}$ and $b = S_0$

Since

$$a < 0, \quad b > 0,$$

the system undergoes a forward bifurcation at $R_0 = 1$

5. Numerical Simulation

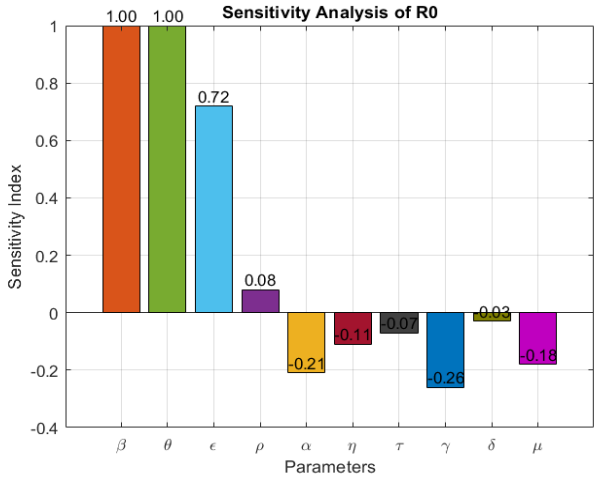

FIGURE 1. Sensitivity index for DFE

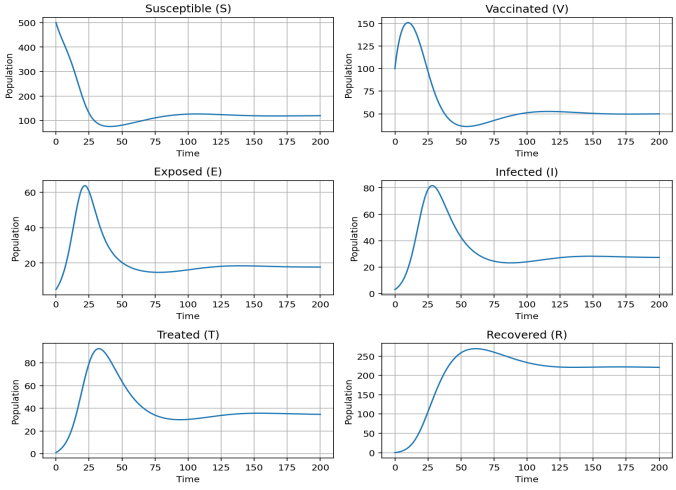

FIGURE 2. Time series analysis for the model for DFE for stability $(R_0 < 1)$

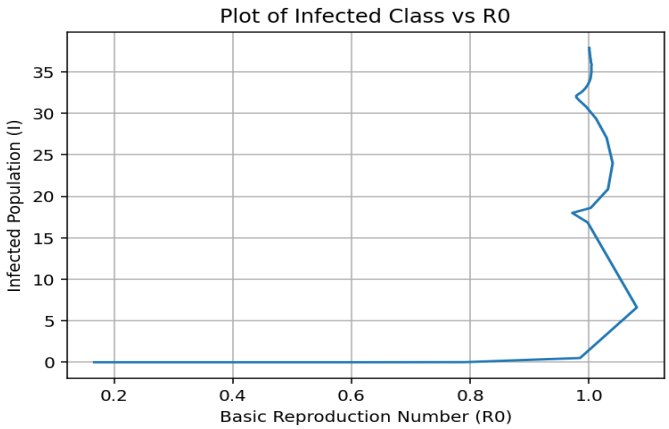

FIGURE 3. Infected behavior for the model for DFE for stability based on (R_0)

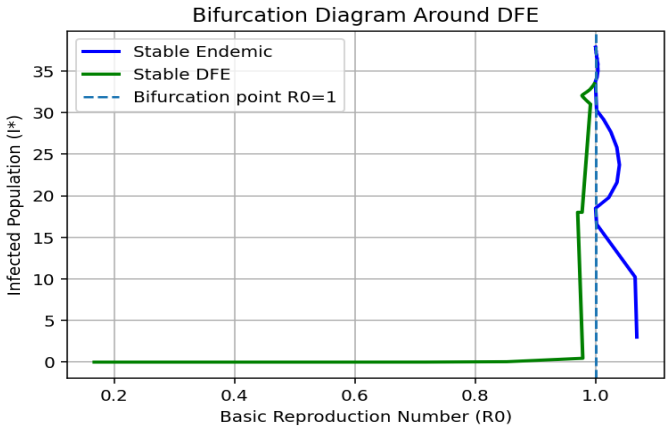

FIGURE 4. Bifurcation diagram for DFE

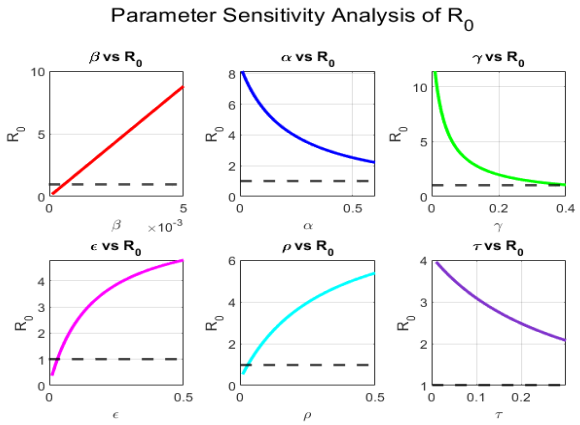

FIGURE 5. Nature of R_0 with respect to different parameters

$$S(0) = 8900000, I(0) = 2, E(0) = 0, T(0) = 0, R(0) = 0, V(0) = 0$$

Parameters	Parametric values
θ	4796.36
β	858×10^{-10}
α	0.000035
η	0.001
ω	0.001
ε	$\frac{1}{6}$
μ	178×10^{-7}
γ	0.000161
ρ	0.05
δ	$\frac{1}{15}$
τ	0.015

TABLE 4. Parametric values used in numerical simulation

We consider a small portion of time in whole $COVID-19$ epidemic so small changes observed in exposed compartments. 3 gives only the significant result to susceptible population.

6. OPTIMAL CONTROL STRATEGY

In order to reduce the spread of the infection and minimize the associated implementation costs, we introduce two time–dependent control variables into the model. The control $u_1(t)$ represents the vaccination effort applied to susceptible individuals, while $u_2(t)$ represents the treatment and testing effort applied to infected individuals.

With the inclusion of these control variables, the controlled epidemic model becomes

$$\begin{aligned}
\frac{dS}{dt} &= \theta + \rho V - \beta SI - (1+u_1(t))\alpha S - \mu S, \\
\frac{dV}{dt} &= (1+u_1(t))\alpha S - \rho V - \mu V, \\
\frac{dE}{dt} &= \beta SI - \eta E - \varepsilon E - \tau E - \mu E, \\
\frac{dI}{dt} &= \varepsilon E - (\gamma + u_2(t))I - \mu I - \delta I,
\end{aligned}$$

$$\frac{dT}{dt} = \eta E + (\gamma + u_2(t))I - \omega T - (\mu + \delta)T,$$
$$\frac{dR}{dt} = \omega T + \tau E - \mu R.$$

The goal is to determine optimal control functions $u_1(t)$ and $u_2(t)$ that minimize the number of infected individuals while keeping the cost of control implementation as low as possible.

The objective functional is defined as

$$J(u_1, u_2) = \int_0^{T_f} \left[AI(t) + \frac{1}{2}\left(B_1 u_1^2(t) + B_2 u_2^2(t)\right) \right] dt, \tag{15}$$

where A represents the weight associated with the infected population and B_1 and B_2 represent the cost coefficients associated with vaccination and treatment strategies respectively.

The optimal control problem consists of finding control functions (u_1^*, u_2^*) such that

$$J(u_1^*, u_2^*) = \min_{(u_1,u_2)\in\Gamma} J(u_1, u_2) \tag{16}$$

subject to the controlled system and the admissible control set

$$\Gamma = \{(u_1, u_2) : 0 \le u_1(t) \le 1,\ 0 \le u_2(t) \le 1,\ t \in [0, T_f]\}. \tag{17}$$

The necessary conditions for optimality are obtained using Pontryagin's Maximum Principle. Accordingly, there exist adjoint variables $\lambda_i(t)$ $(i = 1, \ldots, 6)$ such that the Hamiltonian function is given by

$$\begin{aligned} H = {} & AI + \frac{1}{2}(B_1 u_1^2 + B_2 u_2^2) \\ & + \lambda_1 (\theta + \rho V - \beta SI - (1 + u_1)\alpha S - \mu S) \\ & + \lambda_2 ((1 + u_1)\alpha S - \rho V - \mu V) \\ & + \lambda_3 (\beta SI - \eta E - \varepsilon E - \tau E - \mu E) \\ & + \lambda_4 (\varepsilon E - (\gamma + u_2)I - \mu I - \delta I) \\ & + \lambda_5 (\eta E + (\gamma + u_2)I - \omega T - (\mu + \delta)T) \\ & + \lambda_6 (\omega T + \tau E - \mu R). \end{aligned}$$

The optimal control functions are characterized by

$$u_1^* = \min\left\{1, \max\left(0, \frac{(\lambda_1 - \lambda_2)\alpha S}{B_1}\right)\right\},$$
$$u_2^* = \min\left\{1, \max\left(0, \frac{(\lambda_4 - \lambda_5)I}{B_2}\right)\right\}.$$

These expressions determine the optimal vaccination and treatment strategies required to minimize the infection burden while maintaining cost efficiency.

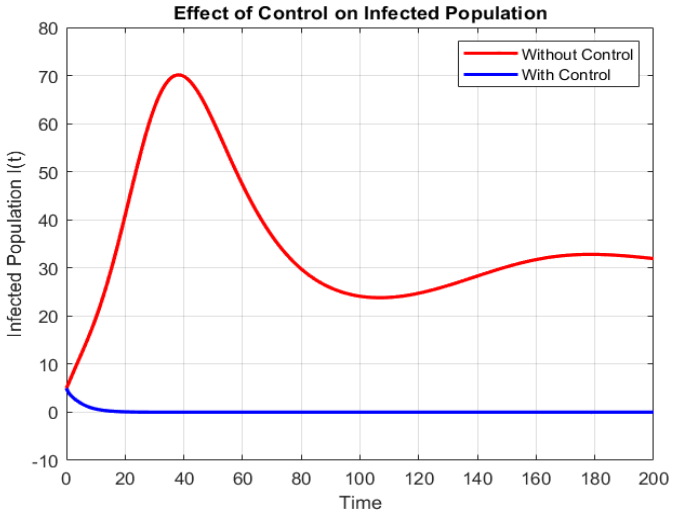

FIGURE 6. Nature of $I(t)$ with and without control

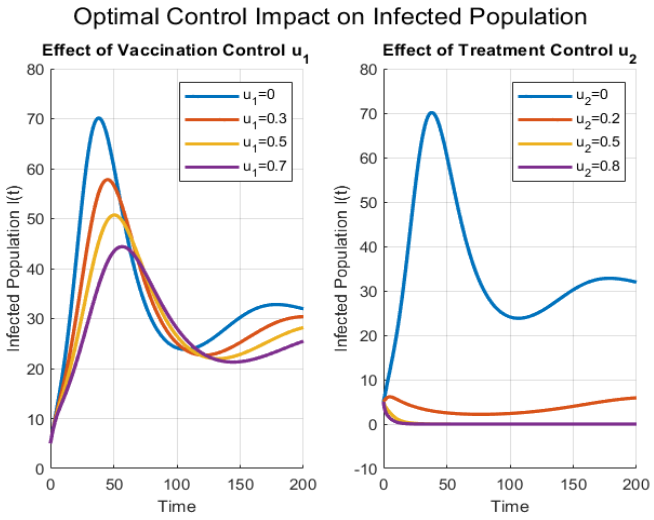

FIGURE 7. Nature of $I(t)$ for different values of control variables

7. Result and Discussion

The sensitivity indices of the basic reproduction number R_0 with respect to the model parameters are illustrated in FIGURE1. Sensitivity analysis provides insight into how variations in parameters influence the transmission dynamics of the disease.

From the figure, the transmission rate β and the recruitment rate θ exhibit the highest positive sensitivity indices, both equal to $+1$. This indicates that R_0 is highly sensitive to these parameters, implying that a proportional increase in either β or θ results in a proportional increase in the value of R_0. The progression rate from exposed to infectious individuals ε also shows a significant positive sensitivity index of 0.72, suggesting that faster progression to the infectious class enhances disease transmission.

On the other hand, several parameters show negative sensitivity indices, indicating their role in reducing disease spread. In particular, the recovery rate γ has the highest negative sensitivity index (-0.26), followed by the vaccination rate α (-0.21) and the natural death rate μ (-0.18). Additionally, the treatment-related parameters η and τ contribute negatively to R_0, although their impact is comparatively smaller.

Overall, the results suggest that reducing the transmission rate β and increasing recovery, treatment, and vaccination-related parameters can significantly reduce the basic reproduction number. Therefore, effective control strategies should focus on limiting disease transmission while enhancing recovery and intervention measures. Numerical simulations are performed to illustrate theoretical results and investigate the impact of different intervention strategies. The simulations demonstrate that combined vaccination and treatment strategies significantly reduce infection levels compared to individual control measures.

In Figure2, The first subplot represents the dynamics of the susceptible population $S(t)$. Initially, the susceptible population starts at a high level and decreases rapidly during the early stage of the epidemic due to infection transmission and vaccination. After a certain period, the susceptible population stabilizes, indicating that the epidemic approaches a steady state.

The second subplot shows the behavior of the vaccinated population $V(t)$. At the beginning, the vaccinated population increases due to the vaccination of susceptible individuals. However,

after reaching a peak, the vaccinated population gradually decreases and stabilizes as individuals either lose immunity or transition to other compartments.

The third subplot illustrates the dynamics of the exposed population $E(t)$. The exposed individuals represent those who have been infected but are not yet infectious. The graph shows that the exposed population increases rapidly during the early phase of the epidemic due to high transmission. After reaching a maximum value, it gradually declines as individuals progress to the infected class or recover through treatment.

The fourth subplot depicts the infected population $I(t)$. The infected population rises significantly during the early phase of disease transmission, reaching a peak around the initial outbreak period. Afterward, the infected population decreases due to treatment, recovery, and control measures incorporated in the model.

The fifth subplot presents the treated population $T(t)$. The treated population increases as infected individuals receive medical treatment. After reaching a maximum value, it decreases gradually as individuals recover and move into the recovered compartment.

The final subplot represents the recovered population $R(t)$. The recovered population steadily increases as infected and treated individuals recover from the disease. Eventually, the recovered population reaches a stable level, indicating the development of immunity within the population.

Overall, the simulation results demonstrate the progression of the epidemic from an initial outbreak to a stabilized state. The graphs clearly highlight the important roles of vaccination and treatment in reducing infection levels and increasing recovery in the population. Figure3 shows a direct correlation between R_0 and infected population size. As R_0 increases from 0.20 to 1.45, infections rise from 1.0 to 3.2. A critical threshold exists at $R_0 = 1.0$, below it, vaccination and exposure dynamics suppress spread, while above it, infections accelerate rapidly, indicating insufficient control measures for higher pathogen transmissibility, which is also visible in Figure4. This sensitivity analysis identifies parameters most influencing R_0, which is described by Figure5. β (transmission rate) shows the strongest positive impact on R_0, while γ (recovery) and ρ (vaccination) exhibit strong negative correlations. ε, α, and η have moderate effects. This highlights that reducing transmission and increasing vaccination are most effective for disease control. Combined control strategies significantly reduce the infected

population over time compared to no intervention, as shown by lower curves as described in Figure6. As noticed in Figure7, higher rate of control u_1 and u_2, drastically reduced the infected population. This demonstrates that increasing both control measures simultaneously provides the most effective epidemic mitigation strategy.

8. Conclusion

This study developed and analyzed a deterministic SVITR compartmental model to understand the transmission dynamics of COVID-19 and evaluate the impact of vaccination and treatment strategies. The model, which incorporates susceptible, vaccinated, infected, treated, and recovered classes, provides a robust framework for assessing intervention measures.

The analysis yielded several key findings. The basic reproduction number (R_0) was derived and shown to be a critical threshold; the disease-free equilibrium is both locally and globally asymptotically stable when $R_0 < 1$. Sensitivity analysis identified the transmission rate (β) as the most influential positive driver of R_0, while the treatment rate (γ) and vaccination-related parameters exhibited strong negative correlations, highlighting their importance for disease control. A bifurcation analysis confirmed that the system undergoes a forward bifurcation at $R_0 = 1$.

Crucially, the optimal control analysis demonstrated that implementing combined time dependent vaccination (u_1) and treatment (u_2) strategies is far more effective in reducing the infected population than single interventions. Numerical simulations confirmed that higher intensities of both controls drastically lower the peak of infections and accelerate epidemic suppression. These results underscore the necessity of integrated public health policies that pair timely vaccination campaigns with effective treatment protocols to mitigate the burden of pandemics like COVID-19.

Conflict of Interests

The authors declare that there is no conflict of interests.

References

[1] S. Raskin, D. Yang, Affine Beilinson-Bernstein Localization at the Critical Level, Ann. Math. 200 (2024), 487–527. https://doi.org/10.4007/annals.2024.200.2.2.

[2] C. Hou, J. Chen, Y. Zhou, L. Hua, J. Yuan, et al., The Effectiveness of Quarantine of Wuhan City against the Corona Virus Disease 2019 (COVID-19): A Well-Mixed SEIR Model Analysis, J. Med. Virol. 92 (2020), 841–848. https://doi.org/10.1002/jmv.25827.

[3] P.V. Markov, M. Ghafari, M. Beer, K. Lythgoe, P. Simmonds, et al., The Evolution of SARS-CoV-2, Nat. Rev. Microbiol. 21 (2023), 361–379. https://doi.org/10.1038/s41579-023-00878-2.

[4] X. Jiang, S. Rayner, M. Luo, Does SARS-CoV-2 Have a Longer Incubation Period than SARS and MERS?, J. Med. Virol. 92 (2020), 476–478. https://doi.org/10.1002/jmv.25708.

[5] W. Guan, Z. Ni, Y. Hu, W. Liang, C. Ou, et al., Clinical Characteristics of Coronavirus Disease 2019 in China, N. Engl. J. Med. 382 (2020), 1708–1720. https://doi.org/10.1056/nejmoa2002032.

[6] M. Lotfi, M.R. Hamblin, N. Rezaei, COVID-19: Transmission, Prevention, and Potential Therapeutic Opportunities, Clin. Chim. Acta 508 (2020), 254–266. https://doi.org/10.1016/j.cca.2020.05.044.

[7] R. Rappuoli, C.W. Mandl, S. Black, E. De Gregorio, Vaccines for the Twenty-First Century Society, Nat. Rev. Immunol. 11 (2011), 865–872. https://doi.org/10.1038/nri3085.

[8] S. Moore, E.M. Hill, L. Dyson, M.J. Tildesley, M.J. Keeling, Modelling Optimal Vaccination Strategy for SARS-CoV-2 in the UK, PLOS Comput. Biol. 17 (2021), e1008849. https://doi.org/10.1371/journal.pcbi.1008849.

[9] K.D. Elgert, Understanding the Immune System, Wiley, 2009.

[10] M. Fudolig, R. Howard, The Local Stability of a Modified Multi-Strain SIR Model for Emerging Viral Strains, PLoS One 15 (2020), e0243408. https://doi.org/10.1371/journal.pone.0243408.

[11] A. Bouchnita, A. Chekroun, A. Jebrane, Mathematical Modeling Predicts That Strict Social Distancing Measures Would Be Needed to Shorten the Duration of Waves of COVID-19 Infections in Vietnam, Front. Public Health 8 (2021), 559693. https://doi.org/10.3389/fpubh.2020.559693.

[12] S.A. Alanazi, M.M. Kamruzzaman, M. Alruwaili, N. Alshammari, S.A. Alqahtani, et al., Measuring and Preventing COVID-19 Using the SIR Model and Machine Learning in Smart Health Care, J. Healthc. Eng. 2020 (2020), 8857346. https://doi.org/10.1155/2020/8857346.

[13] S. He, Y. Peng, K. Sun, SEIR Modeling of the COVID-19 and Its Dynamics, Nonlinear Dyn. 101 (2020), 1667–1680. https://doi.org/10.1007/s11071-020-05743-y.

[14] R. Ghostine, M. Gharamti, S. Hassrouny, I. Hoteit, An Extended SEIR Model with Vaccination for Forecasting the COVID-19 Pandemic in Saudi Arabia Using an Ensemble Kalman Filter, Mathematics 9 (2021), 636. https://doi.org/10.3390/math9060636.

[15] E. Loli Piccolomini, F. Zama, Monitoring Italian COVID-19 Spread by a Forced SEIRD Model, PLoS One 15 (2020), e0237417. https://doi.org/10.1371/journal.pone.0237417.

[16] P. Fonseca i Casas, V. García i Carrasco, J. Garcia i Subirana, SEIRD COVID-19 Formal Characterization and Model Comparison Validation, Appl. Sci. 10 (2020), 5162. https://doi.org/10.3390/app10155162.

[17] S. Athithan, M. Ghosh, Mathematical Modelling of TB with the Effects of Case Detection and Treatment, Int. J. Dyn. Control 1 (2013), 223–230. https://doi.org/10.1007/s40435-013-0020-2.

[18] K. Oshinubi, O.J. Peter, E. Addai, E. Mwizerwa, O. Babasola, et al., Mathematical Modelling of Tuberculosis Outbreak in an East African Country Incorporating Vaccination and Treatment, Computation 11 (2023), 143. https://doi.org/10.3390/computation11070143.

[19] B.C. Agbata, D. Omale, P.B. Ojih, I.U. Omatola, Mathematical Analysis of Chickenpox Transmission Dynamics with Control Measures, Cont. J. Appl. Sci. 14 (2019), 6–23. https://doi.org/10.5281/zenodo.3247243.

[20] P. Fine, K. Eames, D.L. Heymann, "Herd Immunity": a Rough Guide, Clin. Infect. Dis. 52 (2011), 911–916. https://doi.org/10.1093/cid/cir007.

[21] O. Diekmann, J.A.P. Heesterbeek, M.G. Roberts, The Construction of Next-Generation Matrices for Compartmental Epidemic Models, J. R. Soc. Interface 7 (2009), 873–885. https://doi.org/10.1098/rsif.2009.0386.

[22] N.M. Ferguson, D. Laydon, G. Nedjati-Gilani, N. Imai, K. Ainslie, et al. Impact of Non-Pharmaceutical Interventions (NPIs) to Reduce COVID-19 Mortality and Healthcare Demand, Report 9, Imperial College COVID-19 Response Team, London, (2020). https://doi.org/10.25561/77482.

[23] E. Iboi, O. Sharomi, C. Ngonghala, A. Gumel, et al., Mathematical Modeling and Analysis of COVID-19 Pandemic in Nigeria, Math. Biosci. Eng. 17 (2020), 7193–7221. https://doi.org/10.3934/mbe.2020369.